Multi-Component Relaxation Study of Human Brain Using Relaxographic Analysis

Yongmin Chang[1,2], Bong Soo Han[2], Bong Seok Kang[3], Kyungnyeo Jeon[1], Kyungsoo Bae[1], Yong-Sun Kim[1,2], Duk-Sik Kang[1,2]

Purpose : To demonstrate that the relaxographic method provides additional information such as the distribution of relaxation times and water content which are poentially applicable to clinical medicine.

Materials and Methods : First, the computer simulation was performed with the generated relaxation data to verify the accuracy and reliablility of the relaxographic method (CONTIN). Secondly, in order to see how well the CONTIN quantifies and resolves the two different T_1 environments, we calculated the oil to water peak area ratios and identified peak positions of T_1-distribution curve of the phantom solutions, which consist of four centrifugal tubes (10 ml) filled with the compounds of 0, 10, 20, 30% of corn oil and distilled water, using CONTIN. Finally, inversion recovery MR images for a volunteer are acquired for each TI ranged from 40 to 1160 msec with TR/TE=2200/20 msec. From the 3 different ROIs (GM, WM, CSF), CONTIN analysis was performed to obtain the T_1-distribution curves, which gave peak positions and peak area of each ROI location.

Results : The simulation result shows that the errors of peak positions were less in the higher peak (centered T_1=600 msec) than in the lower peak (centered T_1=150 msec) for all SNR but the errors of peak areas were larger in the higher peak than in the lower peak. The CONTIN analysis of the measured relaxation data of phantoms revealed two peaks between 20 and 60 msec and between 500 and 700 msec. The analysis gives the peak area ratio as oil 10%: oil 20%: oil 30%=1:1.3:1.9, which is different from the exact ratio, 1:2:3. For human brain, in ROI 3 (CSF), only one component of -distributions was observed whereas in ROI 1 (GM) and in ROI 2 (WM) we observed two components of T_1-distribution. For the WM and CSF there was great agreement between the observed T_1-relaxation times and the reported values.

Conclusion : we demonstrated that the relaxographic method provided additional information such as the distribution of relaxation times and water content, which were not available in the routine relaxometry and T_1/T_2 mapping techniques. In addition, these additional information provided by relaxographic analysis may have clinical importance.

Index words : Relaxation, Relaxometry, Brain

JKSMRM 6:120-128(2002)

[1]Department of Diagnostic Radiology, College of Medicine,
[2]The Institute of Medical Imaging, College of Medicine, Kyungpook National University
[3]The Biomedical Research Institute, Kyungpook National University Hospital

This work was supported by Biomedical Research Institute Grant, Kyungpook National University Hospital (1997).
Received; September 21,2001, acceepted; July 1, 2002

Address reprint requests to : Yongmin Chang, Ph.D., Department of Diagnostic Radiology, College of Medicine, Kyungpook National University and Hospital, 50 Samduk-dong, Taegu 700-412, Korea.
Tel. 82-53-420-5471, Fax. 82-53-422-2677

Introduction

Magnetic Resonance (MR) has developed into an important imaging modality. Conventional proton MR imaging (MRI) provides information concerning the MR parameters such as proton density, the relaxation times T_1 and T_2, and flow (1). Among them, the relaxation times of proton signal can give important biochemical and/or biophysical information (2, 3). High soft tissue contrast in MRI is known as a direct result of differences in the relaxation times (T_1 and/or T_2) of the different tissues. Proton MR relaxation times in samples of living tissue are the result of complex contributions from different tissue types and different physiological processes. Therefore, it is becoming clear that the quantitative, analytic technique for taking advantage of both relaxation informations and the image contrast may provide better diagnostic information. For example, if a process results in diffuse brain abnormality, such that the entire brain is affected in a subtle way, it is necessary to evaluate images using quantitative methods in addition to image contrast (4, 5).

In this study, we demonstrate that the relaxographic method can be one of most promising techniques for this purpose. This concept was recently introduced by Springer and co-worker (6). Relaxogram describes the probability distribution of spins having different values of relaxation times. That is, the area under the relaxographic peak is directly proportional to the numbers of spins with a given T_i value or a range of T_i values, where i = 1, 2. Therefore, the relaxogram discriminates different T_i and the compositions of each T_i with accuracy. Mathematically, the relaxogram is the form of inverse Laplace transform (ILT) of a relaxation decay data (7). Recently it has also reported that relaxogram will be particularly useful for isochronous signals with more than one relaxation time (8). Thus, combined with MRI, we can principally discriminate the components of relaxation times with their relative fractions in a given area or volume down to the pixel level. This new approach may have a variety of application. In cancer research, relaxogram can be used to monitor tumor growth and the effects of treatment before and after various theraphy. This is based on the observation that NMR relaxation times, both T_1 and T_2, are very sensitive indicator of tumor growth and a sensitive monitor of tumor response to the theraphy (9).

Materials and Methods

a) Computer simulation

In the inversion recovery process, a proton with T_1 and T_2 generates MR signal intensity $I(TI)$:

$$I(TI) \propto (1-2e^{-TI/T_1}+e^{-TR/T_1})\, e^{-TE/T_2} \qquad [1]$$

where TI, TR and TE are inversion time, repetition time and the echo delay time, respectively. The MR signal intensity from a biological sample with continuous T_1 and T_2 distribution are given by the integration with respect to T_1 and T_2. Since, however, the parameter TE is constant, the transverse relaxation time (T_2), can be integrated out. Therefore, the resulting MR signal intensity is expressed by

$$I(TI) = \int_{T_1min}^{T_1max} S(TI, T_1)\, D(T_1)\, dT_1 + \epsilon \qquad [2]$$

with

$$S(TI, T_1) = (1-2e^{-TI/T_1}+e^{-TR/T_1}), \qquad [3]$$

where $D(T_1)$ is proportional to the T_1 relaxation distribution function of the protons and ϵ is the unknown error or noise component. In the following we will call the $D(T_1)$ as T_1 relaxation distribution function for convenince. The $D(T_1)$ can be determined by deconvolution of the equation (2). Mathematically, the equation (2) is ill-posed problem. That is, there are infinitely many possible solutions all satisfying the equation witthin the error ϵ. Using "the principle of parsimony" the program CONTIN developed by Provencher (10, 11) gives the solution of the equation (2) without prior assumptions about the number of exponential components in T_1-relaxation distribution. However, the accuracy and resolving power of the solutions depends on the signal-to-noise ratio (SNR) of the I(TI). Therefore, in this simulation we check the validity of the application of CONTIN to experimental data.

First, T_1 relaxation distribution function, $D(T_1)$, is constructed in a following form:

$$D(T_1) = A\left\{\frac{R}{\sqrt{2\pi\sigma_a^2}}\, e^{-(T_1-T_{1a})^2/2\sigma_a^2} + \frac{(1-R)}{\sqrt{2\pi\sigma_b^2}}\, e^{-(T_1-T_{1b})^2/2\sigma_b^2}\right\} \quad [4]$$

where R is an area ratio of the component centered at T_{1a} and the overall factor A with dimension of $[I(TI)][T]^{-1}$ has constant value of 1500 through the simulation. I(TI) are then generated using equation (2) and (4): with equal spaced interval from $T_{1\,min}$ to $T_{1\,max}$ 30 simulated data points for I(TI) are obtained from equations (2) and (4). For the backgraound noise term, ϵ, 30 data points are randomly generated with normal distribution with zero mean and standard deviation σ_ϵ. The SNR of the simulated data is then defined as $I(0)/\sigma_\epsilon$ and simulation is performed for the case of SNR = ∞, 1000 and 100.

In this simulation, we examine the effect of FWHM (full width at half maximum) of the T_1 relaxation distribution function and the SNR of input data on the accuracy of the solution of the equation (2). For single exponential model, we choose one component T_1 relaxation distribution functoin (R = 1.0) centered at T_{1a} = 600 ms. For the two cases of σ_a = 10 and σ_a = 40 the equation (2) is solved by CONTIN and the simulated σ_a, which is related with FWHM by FWHM = $\sqrt{8\ln 2}\,\sigma_a$, peak positions and peak areas are calculated and compared with original ones.

Secondly, for two components $D(T_1)$ we also examine the effect of SNR of simulated data on the accuracy and resolving power of the solution of CONTIN. Using the parameters T_{1a} = 150, T_{1b} = 600, and $\sigma_a = \sigma_b$ = 30 the simulation is perfomed for R = 0.027, 0.1 and 0.5. We also performed simulation to find out the minimum R (threshold R) for which two peaks can be detected in the solution of Eq. (2). The simulated peak position, peak area and average T_1 are compared with original ones for SNR = ∞, 1000, and 100. We also calculate the peak area among the peaks with R = 0.027, 0.1 and 0.5.

b) Phantom study

To see how well the CONTIN quantifies and resolves the water and oil from a mixture of two, we calculate the oil to water peak area ratios and identify peak positions of T_1-distribution function resulting from CONTIN analysis.

The phantoms, which consist of four centrifugal tubes (10 ml) filled with 0, 10, 20, 30% of corn oil and distilled water, are prepared. To make the homogeneous admixture of the oil and water, the 0.02 (g/ml) of Agar(SAMCHUN CHEMICAL) is added to the mixture. The more the measured T_1 -inversion recovery curve closely reaches the plateau of it, the more accurate solution the CONTIN gives. Therefore, to obtain the inversion recovery curve with plateau for TR ~ 2000 msec, the 0.05% of contrast agent (OMNISCAN, NYCOMED IMAGING AS) is added to shorten the T_1 of distilled water to around 700 msec.

The inversion recovery MR images are acquired by using the 1.5T whole body scanner (Siemens Vision Plus, Siemens Medical, Germany). The inversion recovery pulse sequence employed 38 inversion recovery times (TI) ranged from 40 and 2000 msec and TR/TE = 3000/20 msec. The signal intensity of the fixed region of interest(ROI) in the inversion recovery image at each TI and the measured data were analyzed using the CONTIN.

c) Human study

Inversion recovery MR images for a healthy volunteer (25 year-old woman) were acquired for each TI ranged between 40 to 1160 msec with TR/TE = 2200/20 msec. The 3 ROIs (ROI 1, ROI 2 and ROI 3 are gray matter (GM), white matter (WM) and cerebrospinal fluid (CSF), respectively as shown in Fig. 1. The signal intensity for each ROI at different TI were measured. Analyzing the data using CONTIN, the T_1-distribution functions, which reveal the peak positions and the peak area ratios, were obtained.

Results

1) Simulation

For one component T_1 relaxation distribution function with two different FWHM σ_a = 10, 40 and three different SNR' s, the estimated σ_a, peak positioins, peak areas and average of CONTIN analysis are tabulated in Table 1. The estimated peak positions and average T_1 agree to exact ones within 2% error. The estimated areas of the peak with σ_a = 40 (error $\simeq$ 2%) show better agreement with exact one than that for the $D(T_1)$ with σ_a = 10 (error $\simeq$ 24%). The estimated increases as SNR decreases and the errors of the estimated σ_a are around 200 ~ 300 % and 3 ~ 25 % for σ_a = 10 and σ_a = 40, respectively. Therefore, the FWHM is not a good reference parameter for small SNR(~ 100).

For R = 0.027, 0.1 and 0.5, the SNR dependence of the

simulation for the two component T_1 relaxation distribution functions with $\sigma_a = \sigma_b = 30$ are examined. The Fig. 2-a, 2-b and 2-c show the estimated $D(T_1)$ of CONTIN analysis for R=0.027, 0.1 and R=0.5, respectively. The thin solid curves represent the original $D(T_1)$ and thick dotted, dashed and solid curves represent the $D(T_1)$' s obtained from CONTIN for SNR=∞, 1000 and 100, respectively. The case of R=0.027 is to test the resolving power of CONTIN.

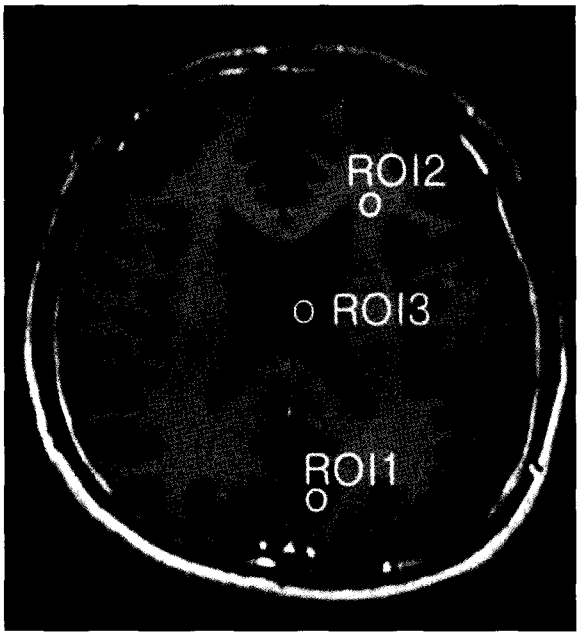

Fig. 1. Three ROIs for relaxographic analysis: ROI 1(GM), ROI 2(WM), and ROI 3(CSF)

That is, it was tested whether CONTIN can distinguish the smaller peak, for which the peak area is only 2.7% of the peak area of the larger peak even with SNR=100. This case is applied to the analysis of the data for human study. For three different R values, the peak positions and peak areas of the curves are tabulated in Table 2. The values for SNR=, 1000 and 100 represent the values resulting from CONTIN analysis. For SNR= ∞ and 1000, the errors of the peak positons and peak areas with R≤0.1 is greater than 10%. As SNR decreases, all estimated positions in two peaks are underestimated for all SNR and the amount of underestimation becomes larger. The estimated peak areas for peak at short T_1 shows the same behavior as the peak positions, however, the estimated peak areas in the peaks at longer T_1 changes from underestimation to overestimatimation as the portion of the peak or SNR decreases.

Since the SNR of the experimental data from a biological sample or a phantom is expected to be around 100, we are interested in the results of SNR=100. The result shows that CONTIN detects the existance of peak down to R=0.027 for SNR=100 but the peak area for small peak (R≤0.1) has very large errors (~40%). However, the peak area ratio is relatively accurate for SNR=100. For R=0.027, 0.1 and 0.5, the area ratio' s of small peak centered at $T_{1a}=150$ msec are 0.05 : 0.15 : 0.58. Therefore, down to R≥0.1, the area ratio, which is resulting from CONTIN

Table 1. For one component T_1 relaxation distribution function with two different FWHM $\sigma_a=10$, $\sigma_b=40$ and SNR, peak positioins, peak areas, average T_1 and the simulated.

SNR	Exact		∞		1000		100	
σ_a	10	40	10	40	10	40	10	40
peak position	600	600	602	595	604	597	612	607
peak area	4300	4300	3250	4233	3249	4230	3244	4223
average T_1 (ms)	600	600	606	600	606	600	614	608
simulated σ_a	10	40	40	50	39	41	29	30

Table 2. The simulated peak positions and peak areas for SNR = infinity, 1000, 100 and R = 0.027, 0.1, 0.5.

	peak positions						peak areas					
	R=0.027		R=0.1		R=0.5		R=0.027		R=0.1		R=0.5	
exact	150	600	150	600	150	600	120	4180	430	3870	2150	2150
SNR=∞	174	608	164	610	157	612	150	4214	474	3885	2261	2148
SNR=1000	179	608	167	613	164	664	160	4208	522	3871	2327	2127
SNR=100	213	630	183	620	167	674	236	4173	606	3801	2486	1989

analysis, seems to reflect the actual ratio of two peaks with accuracy. This result will be applied to the following two cases of phantom and human study.

2) Phantom study

The D{T_1}' s obtained from phantoms are depicted in Fig. 3. The solid curve, which represents pure water, has only one peak at $T_1 = 688$ msec. This short T_1 value is expected because we use the contrast agent to shorten the T_1 of water to $T_1 \simeq 700$. Because water protons experience the same chemical environment, the CONTIN result of single T_1 distribution is quite reasonable. The dotted, dashed, dot-dashed curve represent the D{T_1}' s for 10%, 20% and 30% of oil,

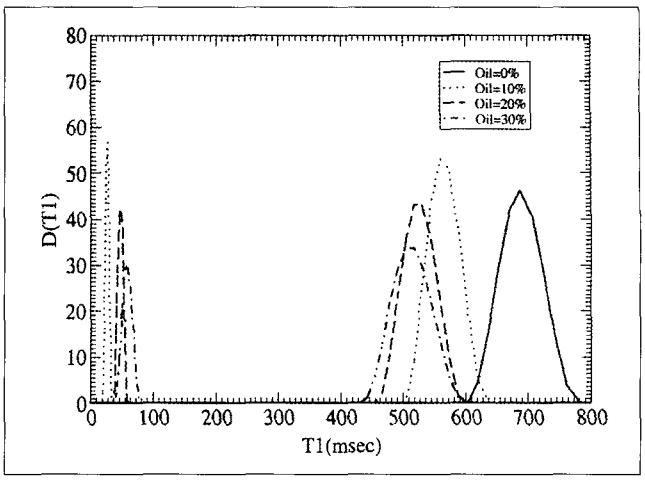

Fig. 3. T_1 relaxation distribution function, D{T_1}, which is estimated using CONTIN, for water-oil phantoms.

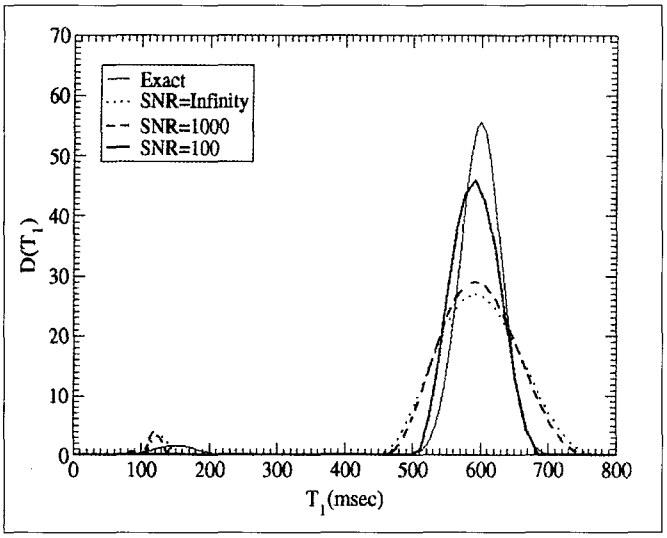

a

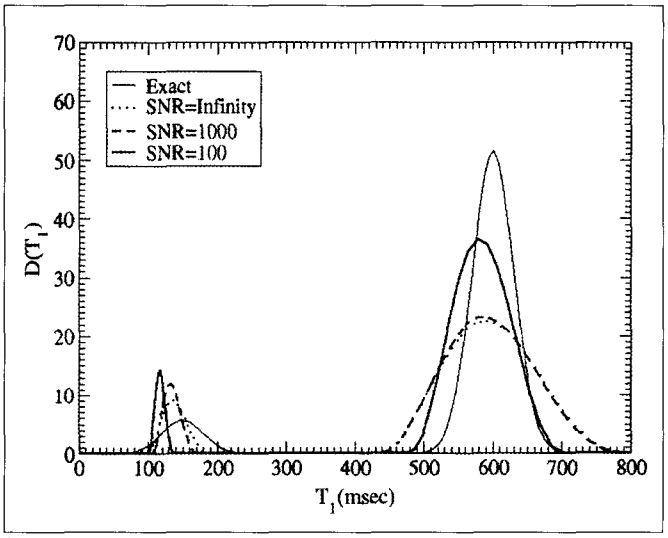

b

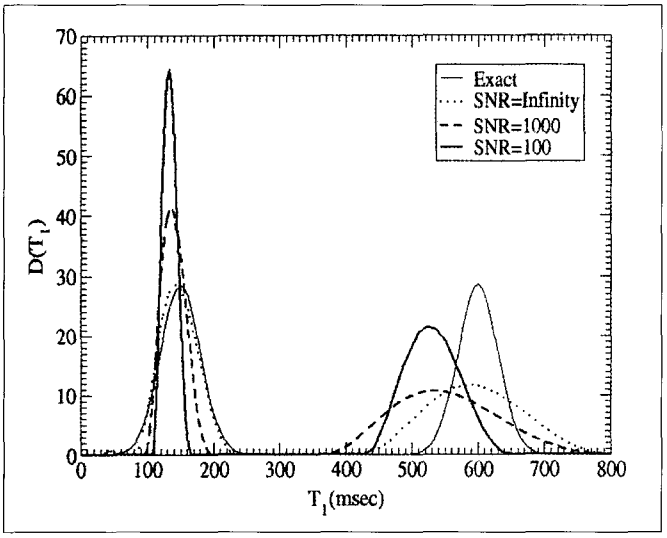

c

Fig. 2. a. The SNR dependency of CONTIN analysis. T_1 relaxation distribution function, D{T_1}, which is estimated using CONTIN, for R= 0.027. **b.** The SNR dependency of CONTIN analysis. T_1 relaxation distribution function, D{T_1}, was estimated using CONTIN, for R= 0.1. **c.** The SNR dependency of CONTIN analysis. T_1 relaxation distribution function, D{T_1}, which is estimated using CONTIN, for R= 0.5.

respectively. They show two peaks between 20 and 60 msec and between 500 and 700 msec. By considering that the oil is mostly lipid, the peaks at shorter T_1's and at longer T_1's are believed to represent the distributions of oil and of water, respectively. These assignments of each peak are further confirmed by observing the increase of peak area of shorter T_1's as the amount of the oil increase.

Since the peak area of oil distribution is proportional to the amount of oil, we evaluate the peak area ratio of phantoms for 10%, 20% and 30% of oil. The peak area ratio was 1 : 1.3 : 1.9, which is different from the nominal ratio, 1 : 2 : 3. There are several possibilities for disagreement. One possibility is the poor homogeneity of the water-oil mixture. Although we used the ultrasound sonicator to make homogeneous mixture, it is quite difficult to obtain completely homogeneous mixture due to hydrophobic nature of lipid. Another possibility is the difference in proton density. There is no reason to assume both water and corn oil have same proton density. If there is a difference, then the nominal ratio might be different from the true ratio because the nominal ratio is the volume ratio of the water and oil. Finally, as shown in Simulation, the error inherent in CONTIN also must be considered.

3) Human study

For human study, the measured data for 3 ROI's are dipicted in Fig. 4. The circles, triangles and stars represent the data for the ROI1, ROI 2 and ROI 3, respectively. T_1-distribution for three ROI's are showed in FIG. 5. The solid, dashed and dot-dashed curves represent the T_1-distribution functions $D(T_1)$ of the ROI 1(GM), ROI 2(WM), and ROI 3(CSF), respectively. In the ROI 3 (CSF), only one component of T_1-distributions is observed whereas in the ROI 1 (GM) and ROI 2 (WM) we observe two components of T_1-distribution. The peak positions of the curves are tabulated in Table 3. For GM and CSF, there are good agreements between the observed T_1-relaxation times and the reported values. On the other hand, the difference between the observed T_1-relaxation time of ROI 2 (WM) and the reported T_1-relaxation time of WM at 1.5T is more than 24%. This discrepancy in T_1-relaxation time of WM seems to result from two major factors. First, to estimate short T1 T_1 of WM, CONTIN requires more data points at short inversion time (TI) although due to the scanner limitation, shortest TI was 40 msec in this study. Secondly, by considering that

Table 3. The T1, peak position, peak area ratio of 3 ROI's resulting from CONTIN analysis for human brain.

	ROI 2(WM))		ROI 1 (GM)		ROI 3(CSF)
Peak Position (msec)	74	650	37	753	2687
Area ratios	4.3%	95.7%	2.8%	97.2%	
Avg. T_1(msec)	631		747		2696
T_1(msec)	510		760		2650
Error	24%		1.7%		1.7%

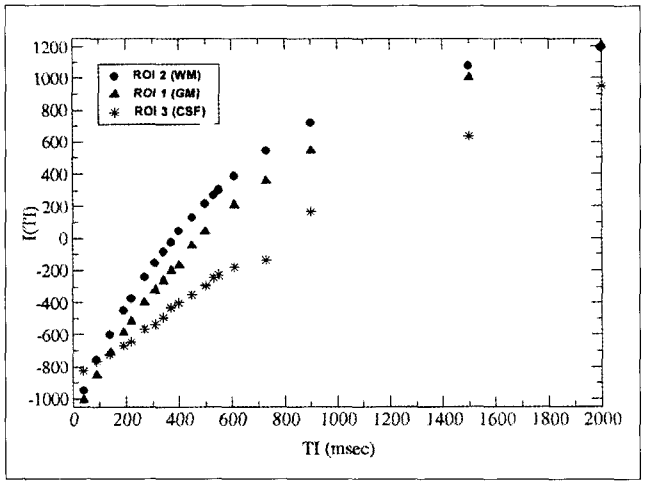

Fig. 4. T_1 recovery curves, which was obtained using inversion recovery sequence for GM, WM, and CSF.

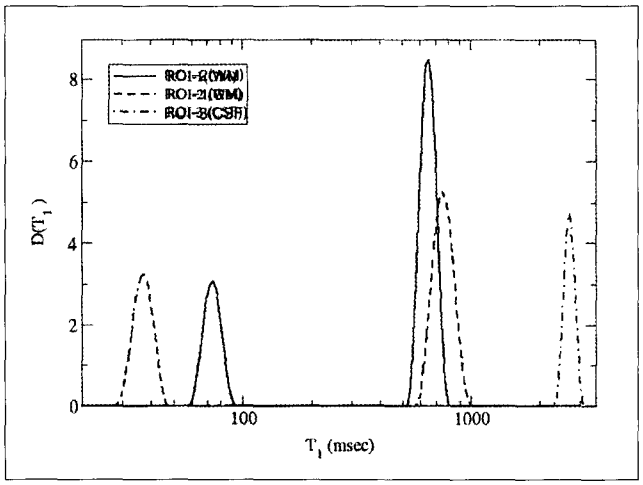

Fig. 5. T_1 relaxation distribution function, $D(T_1)$, which is estimated using CONTIN, for 3 ROI's of human brain.

CONTIN analysis is not reliable for small R($\leq$0.1), the peak area of short T_1 component of WM was too underestimated. Therefore, the average T_1 of WM might be shifted to longer T_1 component of WM. However, it is important that the existence of the small peaks around T_1=74 msec and 37 msec in ROI 1 and ROI 2 seems to suggest multi-exponential behaviors of these tissues. Although the CONTIN analysis shows some error in estimating the peak area ratio, the simulation reveals that CONTIN always resolve the two peak even for small R($\leq$0.1).

Discussion and Conclusion

In this study, it was demonstrated that relaxographic method provides additional informations such as the distribution of relaxation times and water content, which were not available in the conventional relaxometry and T_1/T_2 mapping techniques. Water in a homogeneous environment has the behavior of monoexponential T_1 relaxation. However, for water in an inhomogeneous living system such as brain, there are different T1 times corresponding to different water environments, such as those in myelin layers, cytoplasm, and cerebrospinal fluid. Therefore, it may be true that more specific information about central nervous system (CNS) tissue is available from quantitative analysis of T_1/T_2 relaxation (12, 13). The conventional quantitative analysis of T_1 or T_2 relaxation is often called "relaxometry" or "T_1 or T_2 mapping" in imaging (14, 15). That is, the main interest of these relaxometry or T_1, T_2 mapping studies is to find the monoexponential T_1/T_2 relaxation times themselves.

The relaxographic approach, on the other hand, provides additional information such as the distribution of relaxation times and water content. That is, the relaxographic analysis provides the continuous distribution of relaxation times. From the distribution of relaxation times, the number of relaxation peak represents the different water environment such as intracellular and extracellular water spaces. In addition, the integral of each peak gives the relative water content. From the results of simulation, it is shown that the relaxographic approach, CONTIN, can distingsh different T_1 relaxation time components and can estimate the distribution of each T_1 relaxation time with accuracy. The accuracy of CONTIN analysis is proportional to SNR of relaxation data. That is, the relaxation peak position and peak area resulting from CONTIN analysis are close to the nominal values as SNR of the relaxation data becomes higher. However, even at lower SNR, the different T_1 relaxation time components are always seperated by CONTIN. Our result therefore suggests that CONTIN can evaluate the number of relaxation components without any prior assumption. This observation is further supported by phantom study. The phantom, which consists of oil and water, provides two different T_1 relaxation time components. The CONTIN analysis of the relaxation data of the phantom results in two T_1 relaxation time components. Therefore, the observed multi-exponential relaxation behavior of WM and GM in human brain is less likely to be artifact.

The CONTIN approach to obtain multi-exponential components of relaxation data is theoretically different from the multi-exponential data anlysis adapted by conventional relaxometry. In conventional relaxometry study, to obtain multi-exponential components, the pre-determined relaxation model, which is mono-exponential or double-exponential, is necessary and the experimetal data is fitted to pre-determined relaxation model. That is, one can analyze the same experimental data in either mono- or multi-exponential model. However, CONTIN, which is fundamentally an Inverse Laplace Transform (ILT) technique, adopts a strategy which uses the fewest degree of freedom that are necessary for a given data set. This is the principle of parsiminy. The principle states that of all the possible solutions, the most appropriate solutions are the simplest ones, i.e., the one that may not have all the detail of the true solution, but which contain the detail that is necessary to fit the data. Thus, it allows the analysis to determine the nature of the relaxation components without any a prior assumptions about the nature of these components. In our human study, CONTIN determined that the relaxation behavior of CSF is mono-exponential whereas GM and WM are relaxed in double-exponential form. The mono-exponential relaxation of CSF is well expected because this fluid suppose to have a single biophysical environment. Therefore, without any pre-determined relaxation model, CONTIN seems to provide the most probable relaxation behavior of the tissue.

Whereas it is difficult to find clinical applications of

the relaxometry and/or T_1, T_2 mapping, the recent studies suggest that additional informations provided by relaxographic method may have clinical importance (16). One example is the peak width of relaxation distribution. A previous in vitro study on guinea pig spinal cord and brain showed that the T_2 peak in normal CNS tissue became narrower with increased severity of experimental allergic encephalomyelitis lesions which exhibited parenchymal cellular infiltration, demyelination, and edema. The narrowing of the peak width was explained resulting from the fact that the inflammatory cells, which infiltrated the parenchyma, were relatively uniform in size. This study therefore anticipate that changes in peak width may be indicative of pathology and could potentially be evident before changes on clinical images. The other possible clinical application of the relaxographic approach is the myelin water percentage. In vivo measurement of myelin water content can be important in the clinical management of multiple sclerosis and other white-matter disorders. Previous in vitro and in vivo studies of CNS tissues showed that the water is compartmentalized in myelin (17,18). Especially, short T_2 component of multi-exponential T2 relaxation in white matter has been observed in other in vitro and in vivo studies of CNS tissue. However, it should be noted that a number of in vivo relaxation studies have not observed this short T_2 component (19, 20). Possible reasons for this discrepancy include insufficient sampling of the relaxation decay curve, insufficient signal-to-noise ratio, and use of a different type of T_2 measurement sequence.

In conclusion, we demonstrate that relaxographic method provides additional information such as the distribution of relaxation times and water content, which were not available in the relaxometry and T_1/T_2 mapping techniques. In addition, these additional informations provided by relaxographic analysis may have clinical importance although the further studies will be necessary to verify the detailed clinical applications.

References

1. Pykett IL, Newhouse JH, Buonanno FS. Principles of nuclear magnetic resonance imaging. Radiology 1982; 143:157-168
2. Gersonde K, Felsberg L, Tolxdorff T, Ratzel D, Strobel B. Analysis of multiple T2 proton relaxation processes in human head and imaging on the basis of selective and assigned T2 values. Magn Reson Med 1984; 1:463-477
3. Gersonde K, Tolxdorff T, Felsberg L. Identification and characterization of tissues by T2 selective whole body proton NMR imaging. Magn Reson Med 1985; 2:390-401
4. Poon CS, Henkelman RM. Practical T2 quantification for clinical applications. J Magn Reson Imaging 1992; 2:541-553
5. Larsson HB, Christiansen P, Zeeberg I, Henriksen O. In vivo evaluation of the reproducibility of T2 and T1 measured in the brain of patients with multiple sclerosis. Magn Reson Imaging 1992; 10:579-584
6. Labadie C, Lee JH, Vetek G, Springer CS. Relaxographic Imaging. J Magn Reson B 1994; 105:99-112
7. Overloop K, van Gerven L. NMR relaxation in adsorbed water. J Magn Reson 1992; 100:303-315
8. Kaplan JI, Garroway AN. Homogeneous and inhomogeneous distributions of correlation times: Lineshapes for chemical exchange. J Magn Reson 1982; 49:464-475
9. Kroeker RM, Henkelman RM. Analysis of Biological NMR relaxation data with continuous distributions of relaxation times. J Magn Reson 1986; 69:218-235
10. Provencher SW. A constrained regularization method for inverting data represented by linear algebraic or integral equations. Comput Phys Comm 1982; 27:213-227
11. Provencher SW. A general purpose constrained regularization program for inverting noisy linear algebraic or integral equations. Comput Phys Comm 1982; 27:229-242
12. Whittall KP, MacKay AL. Quantitative interpretation of NMR relaxation data. J Magn Reson 1989; 84:134-152
13. Cheng KH. In vivo tissue characterization of human brain by chi-squares parameter maps: Multiparameter proton T2 relaxation analysis. Magn Reson Imaging 1994; 12: 1099-1109
14. Crawley AP, Henkelman RM. Errors in T2 estimation using multislice multiple-echo imaging. Magn Reson Med 1987; 4:34-47
15. Edelstein WA, Bottomley PA, Pfeifer LM. A signal-to-noise calibration procedure for NMR imaging systems. Medical Phys 1984; 11:180-185
16. Whittall KP, MacKay AL, Graeb DA et al. In vivo measurement of T2 distributions and water contents in normal human brain. Magn Reson Med 1997; 37:34-43
17. Fisher HW, Rinck PA, Haverbeke YV, Muller RN. Nuclear relaxation of human brain gray and white matter: analysis of field dependence and implications for MRI. Magn Reson Med 1990; 16:317-334
18. MacKay AL, Whittall KP, Adler J et al. In vivo visualization of myelin water in brain by magnetic resonance. Magn Reson Med 1994; 31:673-677
19. Ernst T, Kreis R, Ross BD. Absolute quantification of water and metabolites in human brain: I. Compartments and water. J Magn Reson B. 1993; 102:1-8
20. Christiansen P, Toft PB, Gideon P et al. MR-visible water content in human brain: a proton MRS study. Magn Reson Imaging 1994; 12:1237-1244

대한자기공명의과학회지 6:120-128(2002)

Relaxographic 분석법을 이용한 뇌의 다중 자기이완특성에 관한 연구

[1]경북대학교 의과대학 진단방사선과학교실,
[2]경북대학교 의학영상연구소
[3]경북대학교병원 의학연구소

장용민[1,2] · 한봉수[2] · 강봉석[3] · 전경녀[1] · 배경수[1] · 김용선[1,2] · 강덕식[1,2]

목적: 자기공명영상과 자기이완분포 분석법을 통합적으로 이용하는 경우 기존의 자기이완시간 분석기법에서 제공할 수 없었던 자기이완시간의 분포 및 해당 분포의 상대적인 물분자 함유량등의 추가적인 정보를 제공할 수 있음을 보이고자 하였다.

대상 및 방법: 자기이완분포 분석법(CONTIN)의 정확도 및 신뢰성을 검증하기 위하여 먼저 자기이완시간이 일정한 분포를 가지도록 고안된 모의 자기이완 데이터를 사용하였다. 다음으로 지질의 함유량이 99% 이상인 식용유와 증류수를 일정비율(0, 10, 20, 30%)로 혼합한 실험 팬텀을 제작하고 inversion-recovery 시퀀스 (TI: 40 -1160 msec, TR/TE=2200/20 msec)를 사용하여 MR 영상을 획득하여 CONTIN을 사용하여 분석하였다. 그리고 사람의 뇌 영상에서 뇌척수액, 백질, 회백질에 관심영역을 설정하고 CONTIN을 사용하여 각 관심영역에서의 자기이완분포를 분석하였다.

결과: 신호대잡음비를 달리한 모의 자기이완 데이터의 분석결과 자기이완시간의 위치에 대한 오차는 신호대잡음비에 관계없이 긴 자기이완시간 (T_1=600 msec)에 비해 짧은 자기이완시간 (T_1=150 msec)에서 크게 나타났으며 반대로 자기이완시간 분포면적에 대해서는 긴 자기이완시간 (T_1=600 msec)의 면적오차가 짧은 자기이완시간 (T1=150 msec)에 비해 큰 것으로 나타났다. 실험 팬톰을 이용한 분석결과는 실제 오일대 증류수의 비율을 1: 2: 3으로 한 팬톰들에서 분석결과는 1 : 1.3 : 1.9으로 나타났다. 자원자의 뇌영상에서는 CSF의 경우에는 하나의 T_1 자기이완시간만이 나타난 반면 백질과 회백질에서는 2개의 T1 자기이완분포를 가지는 것으로 분석되었다. CSF와 백질의 평균 자기이완시간은 기존의 보고된 값들과 잘 일치 하였다.

결론: 자기공명영상과 자기이완분포 분석법을 통합적으로 이용하는 경우 기존의 자기이완시간 분석기법에서 제공할 수 없었던 자기이완시간의 분포 및 해당 분포의 상대적인 물분자 함유량등의 추가적인 정보를 제공한다는 사실을 규명하였고 이러한 추가적인 정보들은 임상적 유용성이 있을 것으로 추정된다.

통신저자 : 장용민, 대구광역시 중구 삼덕동 50 경북대학교병원 진단방사선과
Tel. (053) 420-5471, Fax. (053) 422-2677